

# Outer Membrane Protein F Stabilised with Minimal Amphipol Forms Linear Arrays and LPS-Dependent 2D Crystals

Wanatchaporn Arunmanee · J. Robin Harris ·  
Jeremy H. Lakey

Received: 13 December 2013 / Accepted: 11 February 2014 / Published online: 1 March 2014  
© The Author(s) 2014. This article is published with open access at Springerlink.com

**Abstract** Amphipols (APol) are polymers which can solubilise and stabilise membrane proteins (MP) in aqueous solutions. In contrast to conventional detergents, APol are able to keep MP soluble even when the free APol concentration is very low. Outer membrane protein F (OmpF) is the most abundant MP commonly found in the outer membrane (OM) of *Escherichia coli*. It plays a vital role in the transport of hydrophilic nutrients, as well as antibiotics, across the OM. In the present study, APol was used to solubilise OmpF to characterize its interactions with molecules such as lipopolysaccharides (LPS) or colicins. OmpF was reconstituted into APol by the removal of detergents using Bio-Beads followed by size-exclusion chromatography (SEC) to remove excess APol. OmpF/APol complexes were then analysed by SEC, dynamic light scattering (DLS) and transmission electron microscopy (TEM). TEM showed that in the absence of free APol–OmpF associated as long filaments with a thickness of ~6 nm. This indicates that the OmpF trimers lie on their sides on the carbon EM grid and that they also favour side by side association. The formation of filaments requires APol and occurs very rapidly. Addition of LPS to OmpF/APol complexes impeded filament formation and the trimers form 2D sheets which mimic the OM. Consequently, free APol is undoubtedly required to maintain the homogeneity of OmpF in solutions, but ‘minimum APol’

provides a new phase, which can allow weaker protein–protein and protein–lipid interactions characteristic of native membranes to take place and thus control 1D–2D crystallisation.

**Keywords** OmpF · Lipopolysaccharides · Amphipol · Transmission electron microscopy · Dynamic light scattering · SEC

## Introduction

*Escherichia coli* are gram-negative bacteria which are a normal but minor commensal in the human gut. Most *E. coli* strains are harmless to humans, however, some strains can cause food poisoning, meningitis, or septicaemia. Like all gram-negative bacteria, the cell envelope of *E. coli* is surrounded by two membranes. The additional, so called outer membrane (OM), is highly asymmetric, consisting of tightly-packed lipopolysaccharides (LPS) located in the outer leaflet and phospholipids located in the inner leaflet. This OM acts as a defensive barrier but is also extremely permeable as a result of a large number of channel-forming proteins associated with the OM (Rosenbusch 1974; Jaroslawski et al. 2009). The nonspecific channel-forming proteins in the OM are termed porins and are responsible for the influx of hydrophilic solutes and nutrients, as well as the excretion of waste products (Nakae 1976; Nikaido 2003). Outer membrane protein F (OmpF) which is the major porin of *E. coli* OM is a trimeric protein, each monomer forming a 16-stranded  $\beta$ -barrel channel which allows the diffusion of small hydrophilic molecules of less than ~600 kDa through its channel across the hydrophobic OM (Cowan et al. 1992). OmpF is also a receptor and a translocator of colicins, bacterial toxins

W. Arunmanee · J. R. Harris · J. H. Lakey (✉)  
Institute for Cell and Molecular Biosciences, Newcastle  
University, Framlington Place, Newcastle upon Tyne NE2 4HH,  
UK  
e-mail: jeremy.lakey@ncl.ac.uk

J. R. Harris  
Institute of Zoology, University of Mainz, 55099, Mainz,  
Germany

produced by *E. coli* (Evans et al. 1996; Cascales et al. 2007). Therefore, OmpF is a potential target for the design of new antibiotics (Johnson et al. 2013).

To study membrane proteins (MP) *in vitro*, they require detergents to stabilise them in aqueous solutions whilst remaining as native structures. It is often a demanding task to find suitable detergents to stabilise MPs outside their lipid bilayer environment. This partly explains why, relative to soluble proteins, so few high-resolution unique structures of MPs have been resolved (White 2009). To provide an alternative technology to overcome this problem, Popot and colleagues developed a novel class of detergent called *Amphipol* (APol), an amphipathic polymer comprising a hydrophilic backbone randomly grafted with hydrophobic chains. This structure enables APol to stabilise MP in detergent-free aqueous solutions (Tribet et al. 1996; Popot 2010). As APol forms multiple contacts with hydrophobic surface of MP, the rate of dissociation of APol from proteins is slow (Popot et al. 2003). Theoretically, APol can solubilise MPs in a near absence of free APol (Tribet et al. 1997; Popot et al. 2003). Since its introduction almost 20 years ago, the reconstitution of MP into APol has become a promising approach to investigate the structure and function of MP. To date, structural studies on several MP stabilised by APol have been carried out using biophysical techniques such as electron microscopy (EM) (Tribet et al. 1998; Flötenmeyer et al. 2007; Gohon et al. 2008; Althoff et al. 2011; Cvetkov et al. 2011; Cao et al. 2013; Liao et al. 2013), nuclear magnetic resonance (NMR) (Zoonens et al. 2005; Catoire et al. 2010) and small-angle neutron scattering (Gohon et al. 2008).

However, although the multiple contacts of APol to MP ensure the high affinity of APol association, less is known about the importance of free APol to the long-term stability of MP APol complexes. Unexpectedly, Zoonens et al. (2007) reported that the removal of free APol gave rise to the association of MP/APol complexes from an initially homogenous state. Likewise, the preparation of bacteriorhodopsin/APol complexes using an approach which completely removed free APol, led to the self-organisation over months or years of bacteriorhodopsin/APol particles into long filaments. This worm-like structure observed by EM was constructed by linear association of monomeric particles (Gohon et al. 2008).

Here, we report our observations of OmpF in complex with APol A8-35 in the absence of free APol. Initially, OmpF/APol complexes were prepared with the aim to study the interaction of the bacterial toxin Colicin N with OmpF (Clifton et al. 2012). However, in the absence of APol, the OmpF/APol complexes had a tendency to form long filaments, similar to those observed by Gohon et al. (2008) for bacteriorhodopsin but much more rapidly. Consequently, we studied the structure and assembly

kinetics of these filaments by transmission electron microscopy (TEM) and dynamic light scattering (DLS). The effect of the OM specific lipopolysaccharide on the self-association of the OmpF/APol complexes was also examined.

## Materials and Methods

Chemicals Specialist chemicals were purchased from the following suppliers octyl-polyoxyethylene (POE); Enzo, R<sub>a</sub>-Lipopolysaccharide (R<sub>a</sub>-LPS); Sigma Aldrich, Bug-Buster protein extraction reagent; Novagen, *n*-dodecyl- $\beta$ -D-glucopyranoside (DG); Anatrace, and *n*-dodecyl- $\beta$ -D-maltoside; Melford. Bio-Beads SM2 were from Bio-Rad. Amphipol A8-35 (APol) was a kind gift from J.L. Popot.

### Expression and Purification of Wild-Type OmpF

Wild-type OmpF was produced from *E. coli* BE3000. Cells were grown in LB (Luria–Bertani) medium in a 10-l Bioflo 3000 bioreactor (New Brunswick Scientific) and growth was monitored by measuring OD<sub>600</sub>. When OD<sub>600</sub> reached 10.0–15.0, cells were harvested by centrifugation at 8,000 $\times$ g at 4 °C for 10 min. WT OmpF was purified as described previously by (Lakey et al. 1985). OmpF was then precipitated in cold ethanol and resuspended in 20 mM sodium phosphate, pH 7.9, 100 mM NaCl, 0.5 % (v/v) octyl-POE.

### Expression and Purification of OmpF Inclusion Bodies

OmpF inclusion bodies were overexpressed from *E. coli* BZB1107 with the plasmid pMS119 in which the *ompF* signal sequence (residues 1–22) plus the initial alanine residue are replaced by a single methionine residue (Visudtiphole et al. 2005). Transformed cells were grown at 37 °C in LB medium in flasks supplemented with 0.05 % (w/v) glucose, 100  $\mu$ g/ml Ampicillin and 30  $\mu$ g/ml Kanamycin. When OD<sub>600</sub> reached 0.6, isopropyl  $\beta$ -D-1-thiogalactopyranoside was added to give a final concentration of 1 mM. After incubation at 37 °C for 3 h, cells were harvested by centrifugation at 8,000 $\times$ g at 4 °C for 10 min. Inclusion bodies were purified using BugBuster protein extraction reagent, solubilised with the denaturation buffer (50 mM sodium phosphate, pH 8.0, 300 mM NaCl, and 6 M guanidinium HCL) and dialysed into 50 mM sodium phosphate, pH 8.0, 300 mM NaCl, and 6 M urea at room temperature.

### Refolding OmpF in Mixed Detergents

The OmpF from solubilised inclusion bodies was refolded by a 20 $\times$  dilution in 50 mM Tris/HCl, pH 8.0, 1 mM

dithiothreitol and 0.1 mM EDTA containing a mixture of 1 % (w/v) *n*-dodecyl- $\beta$ -D-glucopyranoside (DG) and 0.4 % (w/v) *n*-dodecyl- $\beta$ -D-maltoside (DM) following the procedure of Visudtiphohle et al. 2005 with some changes. After incubation at 37 °C for 3 days, the refolding buffer was exchanged with 20 mM Tris/HCl, pH 7.4, 0.5 % (v/v) octyl POE, on 1-ml HiTrap Q Sepharose column. OmpF was then precipitated in cold ethanol and resuspended in 20 mM sodium phosphate, pH 7.9, 100 mM NaCl, 0.5 % (v/v) octyl-POE.

#### Reconstitution of OmpF into Amphipol A8-35

The reconstitution of OmpF into APol was carried out as previously described by Zoonens et al. 2005. APol A8-35 was added to OmpF in 20 mM sodium phosphate, pH 7.9, 100 mM NaCl, 0.5 % (v/v) octyl-POE at 1:10 protein/APol weight ratio. After incubation for 15 min at room temperature, the wet polystyrene beads (Bio-Beads SM2), pre-washed with methanol and water, were added to remove octyl-POE at a 1:10 detergent/beads weight ratio and then incubated for 2 h at room temperature on a roller mixer. The beads were removed by using an Eppendorf 5424 benchtop microcentrifuge at maximum speed for 1 min.

#### Lipopolysaccharide Preparation

R<sub>a</sub>-LPS was dissolved in 20 mM sodium phosphate, pH 7.9, 100 mM NaCl to give a final concentration of 2 mg/ml. The LPS solution was then sonicated in a water bath for 20 min and temperature cycled 6 times between 4 and 70 °C. The resulting solution was kept at 4 °C overnight before use.

#### Size-Exclusion Chromatography

Size-exclusion chromatography (SEC) was performed using an ÄKTA purification system (GE Healthcare). All buffers were filtered through a 0.22  $\mu$ m filter and 100  $\mu$ l samples were injected into a Superose 12 10/300 GL column which was previously equilibrated with 20 mM sodium phosphate, pH 7.9, 100 mM NaCl until a stable baseline was reached. Elution at a flow rate of 0.5 ml/min was carried out at room temperature and the proteins were detected using optical absorption at 280 nm.

#### Dynamic Light Scattering

DLS measurements were carried out using a Zetasizer Nano (Malvern instrument Ltd.) on 50  $\mu$ l samples at 0.1–0.5 mg/ml OmpF in a quartz cuvette (Hellma 105.251-QS) at 30 °C. The size measurements and the data analysis were carried out using Zetasizer software.

#### Transmission Electron Microscopy

Negatively stained specimens were prepared using the single-droplet Parafilm procedure as described in (Harris 1997). Samples were adsorbed to glow-discharged carbon-coated grids and individually negatively stained with uranyl acetate (2.0 % w/v). After 30-s incubation, the excess of protein, washing and staining solution was blotted away with filter paper (Whatman No.1), and the grids air dried for a further 1–2 s. Electron micrographs were recorded at 100 kV from a Philips CM100 transmission electron microscope as digital images, using an Optronics 1824  $\times$  1824 pixel CCD camera with an AMT40 version 5.42 image capture engine, supplied by Deben UK. From the calibrated images, feature sizes were determined within JMicroVision v1.27.

## Results and Discussion

### OmpF/APol Complexes Associate as Filaments in the Absence of Free APol

Native trimeric OmpF purified from *E. coli* OM was reconstituted into Amphipol 8-35 at a ratio of 1 OmpF/10 APol by weight (since the MW of an A8-35 polymer is approximately 4.3 kDa and the MW of OmpF is 37 kDa this ratio is roughly a 1 OmpF/100 APol molar ratio). The size and dispersity of the OmpF–APol complexes were then analysed by SEC in APol-free buffer. The SEC elution profiles shown in Fig. 1a indicated that the OmpF/APol complexes exiting the column were virtually monodisperse with a very small amount of aggregate, which eluted at the void volume. When comparing the SEC chromatogram of OmpF/APol complexes to that of OmpF/octyl-POE complexes eluted in octyl-POE containing buffer, the OmpF/APol particles eluted at 9.1 ml, while OmpF/octyl-POE complexes eluted at 9.8 ml indicating that the OmpF/APol particles are slightly larger than OmpF in octyl-POE.

The OmpF/APol complexes taken from the main peak were presumably free of unbound APol, but the final ratio of the two components in this sample is unknown. These complexes were negatively stained and then studied by TEM. According to the published high-resolution structure of OmpF, illustrated in Fig. 1b (Cowan et al. 1992), OmpF forms a trimer with a height of approximately 6 nm and a maximum diameter of about 10 nm. Since the SEC elution profile revealed a homogeneous population of OmpF–APol complexes marginally larger in diameter than detergent solubilised trimers, the negatively stained TEM images of OmpF/APol complexes were expected to reveal evenly dispersed single particles on the carbon film. Surprisingly, the electron micrographs (Fig. 1c) demonstrated that

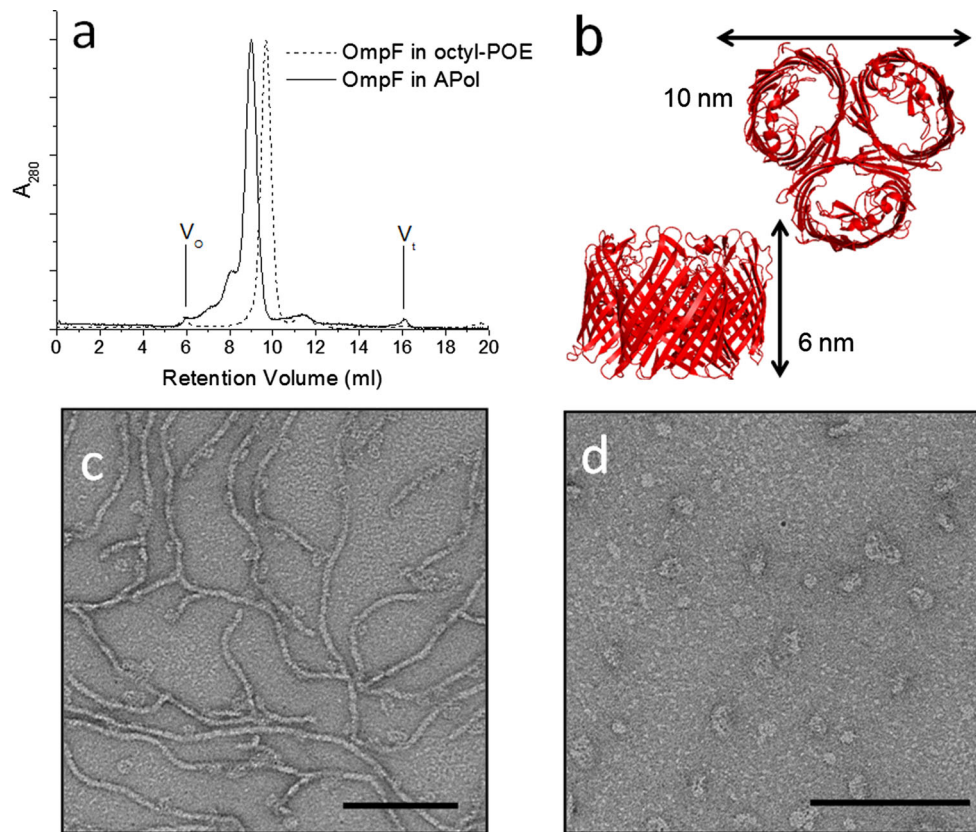


**Fig. 1** Removal of free APol by SEC leads to the formation of OmpF/APol filaments. **a** The comparison of size and dispersity between OmpF prepared in APol 1:10 OmpF/APol mass ratio (*solid line*) and OmpF in 0.5 % (v/v) octyl POE (*dash line*). OmpF/APol complexes were injected onto Superose 12 column equilibrated with detergent-free buffer, while buffer containing octyl-POE was used for OmpF/octyl-POE samples. Profiles have been normalised to the same maximum. **b** Top and side view of crystal structure of OmpF trimer

(PDB code: 2OMPFF). The diameter and height of OmpF are about 10 and 6 nm, respectively. Electron micrographs of negatively stained OmpF/APol complexes. **c** OmpF/APol filaments formed 1 day after removal of free APol by SEC. **d** The same batch of complexes after supplementing with free APol at 1:5 OmpF/APol mass ratio. Addition of free APol resulted in dissociation of the filaments. Scale bars 100 nm

OmpF/APol complexes formed long filaments with a characteristic width of  $\sim 6$  nm. This width corresponds to the minimum dimension of OmpF, the height of the trimer, and suggests that they absorbed edge-on to the carbon film. Thus, the width of the filaments is rather constant, whereas, in contrast, the length of the long filaments is highly variable. The characteristic three pores which traverse the OmpF trimer show up as stain filled pits in negatively stained TEM images but were rarely seen within the filaments, thus supporting the suggestion that the hydrophobic edge of the filament preferentially absorbs onto the carbon film. OmpF without detergent forms large aggregates, so APol must still be present and involved in the filament structures which are stable in solution for at least a week with a complete absence of aggregates seen after centrifugation. Furthermore, filament formation by OmpF/APol complexes is reversed when adding free APol at 1:5 OmpF/APol weight ratio back to the same batch of OmpF/APol complexes containing filaments (Fig. 1d).

#### LPS Inhibits Self-Association of OmpF/APol Complexes

Conventionally expressed, *in vivo* folded, OmpF is purified from the OM of *E. coli* which contains tightly-packed LPS in the outer leaflet. OmpF extracted from this membrane often co-purifies with the significant amounts of tightly bound LPS. This OmpF–LPS interaction is stable enough to be observed by SDS-PAGE analysis of native OmpF trimers and reveals a ladder pattern of LPS-bound OmpF bands (Fig. 2a) (Baboolal et al. 2008). The number of additional bands indicates the relative amount of LPS attached to the OmpF trimers. In the initial study, above, the samples had a low LPS content but were not conclusively LPS free. Since LPS molecules cross-link to adjacent LPS via divalent cations such as  $\text{Ca}^{2+}$  and  $\text{Mg}^{2+}$  (Schneck et al. 2010), the OmpF–LPS interaction may promote lateral OmpF association. In order to clearly investigate the effect of LPS on the formation of filaments,



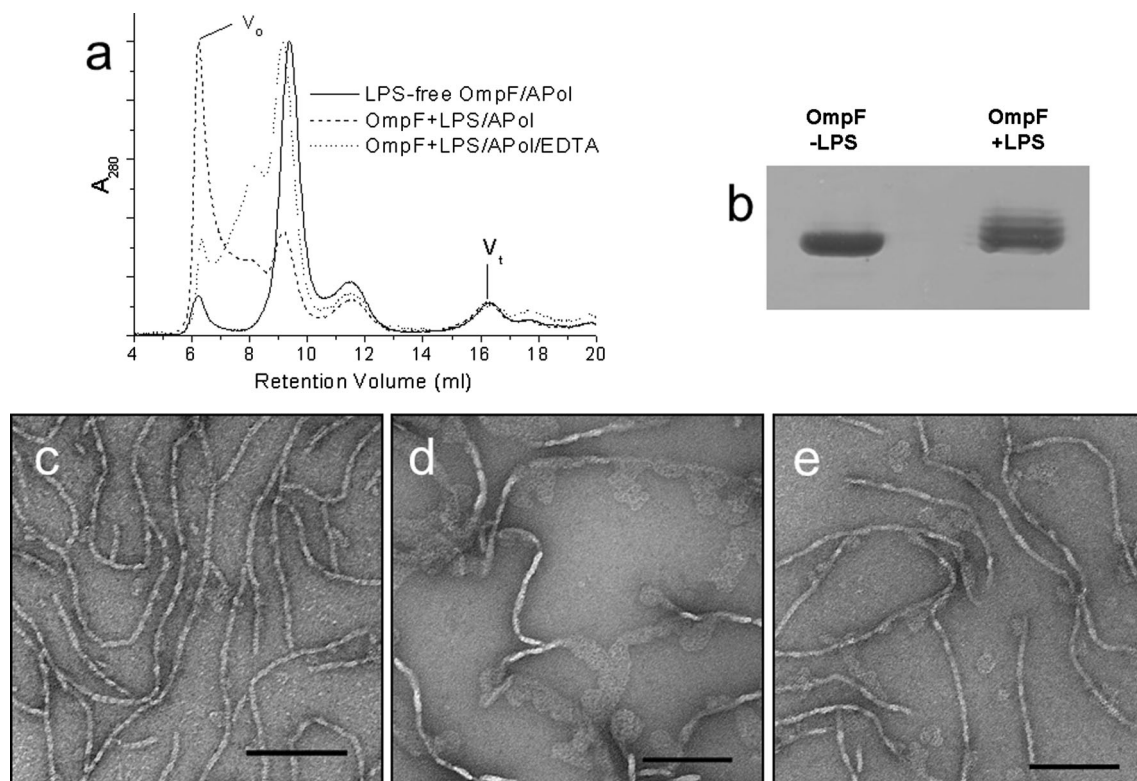


**Fig. 2** Effect of lipopolysaccharides on the structure of OmpF/APol complexes. **a** SEC analysis of size and homogeneity of OmpF/APol complexes in various conditions. (*Solid line*) LPS-free OmpF, (*dashed line*) OmpF+LPS, (*dotted line*) OmpF+LPS in 1 mM EDTA. In each case, the column was pre-equilibrated with detergent-free buffer. Profiles have been normalised to the same maximum. **b** SDS-PAGE

analysis of LPS-free OmpF versus OmpF with added LPS showing characteristic ladder of OmpF bands resulting from LPS binding. The number of additional bands represents the increasing number of LPS attached to OmpF. EM study of OmpF/APol complexes in the presence and absence of LPS. **c** LPS-free OmpF/APol. **d** OmpF+LPS/APol. **e** OmpF+LPS/APol/EDTA. Scale bars 100 nm

LPS-free OmpF was produced by refolding OmpF from denatured inclusion bodies. In the present study, LPS-free OmpF, OmpF+LPS and OmpF+LPS in EDTA were reconstituted into APol, and the complexes were fractionated by SEC. We used 'rough' Ra-LPS lacking the outer core and O-antigen to limit the interactions to the membrane region of OmpF and this was added to LPS-free OmpF at 1:5 OmpF/LPS molecular ratio prior to incubation with APol. The addition of 1 mM EDTA removed divalent cations from the buffer to inhibit LPS–LPS association. According to SEC elution profiles shown in Fig. 2b, LPS-free OmpF/APol complexes appeared to be monodisperse with a small amount of aggregate present, whereas the bulk of the OmpF+LPS/APol sample eluted as large aggregates at the void volume. Furthermore, when OmpF+LPS/APol complexes were formed in, and eluted in SEC column buffer containing EDTA, the amount of aggregates significantly decreased leaving a mixture of OmpF/APol particles with various sizes.

The structure of OmpF/APol complexes was further studied by TEM. Using LPS-free OmpF, the filaments of OmpF/APol still appeared in the absence of free APol

(Fig. 2c). However, they clearly showed a beaded structure which probably corresponds to the repetitive pattern of OmpF trimers along the chain. OmpF/APol complexes in the presence of LPS assembled as sheet-like structures rather than filaments (Fig. 2e) and this led to small areas of apparent 2D crystallisation. In fact, the filament-like structure observed in samples of OmpF+LPS/APol were, in reality, folded sheets of OmpF. Once divalent cations were chelated by EDTA, a combination of small sheet-like and filamentous structure was observed (Fig. 2d). These results indicate that LPS disrupts the linear (1D) filaments of OmpF stabilised by APol and provokes a 2D behaviour reminiscent of the natural membrane and also in vitro crystals formed by OmpF–Lipid mixtures (Hoenger et al. 1993b; Schabert and Engel 1994; Baboolal et al. 2008). Thus, the OmpF/APol structure stabilises a unique interaction where a simple, side by side, linear association of trimers is preferred over all other forms. However, this stability is easily disrupted by LPS to form 2D sheets or by excess APol to form isolated complexes. In the presence of a carbon grid surface used for EM it appears that one membrane face of the linear filament, normally stabilised

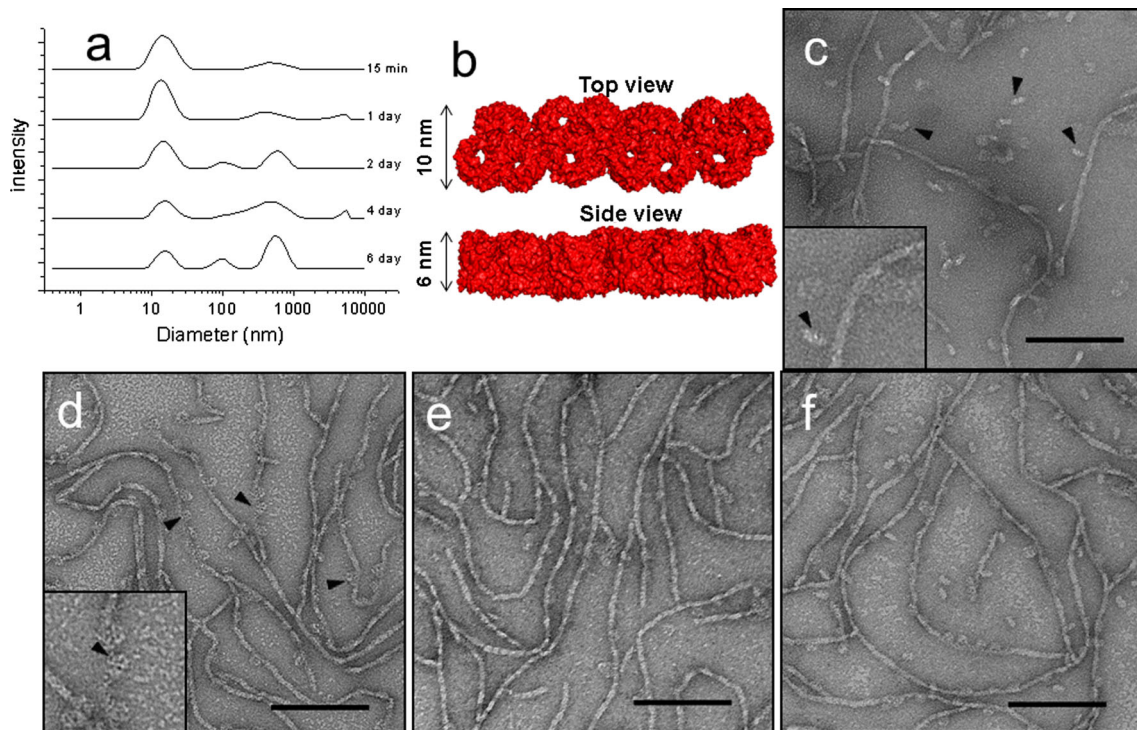


**Fig. 3** Progression of filament formation by OmpF/APol complexes. **a** Size distribution of OmpF/APol complexes by intensity measured at 30 °C by DLS from 15 min to 6 days after SEC. **b** Structural models of possible OmpF filaments showing ‘top’ and ‘side’ views. Electron microscopy of OmpF/APol studied at different times after SEC.

**c** After 10 min. Single particles of OmpF trimer (*arrowheads*) were present. **d** After 10 min. OmpF pores (*arrowheads*) can be seen on filaments. **e** After 1 day. **f** After 1 week. Scale bars 100 nm. The insets in **c**, **d** are at  $\times 2$  higher magnification

by APol, is adsorbed onto that surface. Thus, the APol–OmpF filaments are marginally stable and highly dynamic such that they can be influenced by small changes in their environment. They may thus be useful starting points for crystallisation studies of OmpF complexes.

#### Maturation of OmpF/APol Filaments

In the previous experiments, all complexes for TEM study were prepared the day before, and thus the rate of formation of OmpF/APol complexes was unknown. To measure the kinetics of OmpF/APol filament formation after the removal of free APol, the size distribution of LPS-free OmpF/APol complexes after SEC was monitored by DLS at 30 °C as a function of time. The size distributions were analysed by intensity as this mode is more sensitive to large particles in the samples. The size of OmpF trimer in conventional detergents measured by DLS is approximately 10 nm (data not shown). DLS size distribution data of OmpF/APol complexes suggested that the number of particles with sizes above 10 nm increased over time while the number of single OmpF trimers/APol decreased (Fig. 3a). Even though we measured freshly prepared complexes, a small amount of large particles was already present after

15 min. Therefore, it is evident that self-association of OmpF in the absence of free APols occurred very rapidly.

The findings from the DLS experiment are in a good agreement with an electron microscopic study on LPS-free OmpF/APol complexes. The images of negatively stained complexes were recorded at different times after SEC. The TEM images of freshly prepared complexes 10 min after filament removal of APol by SEC revealed that there was the mixture of short and long filaments, as well as individual particles of OmpF trimers (Fig. 3c, d). Groups of OmpF trimers starting to join up with the filaments can also be observed in these early samples. Interestingly, the top view of OmpF, with stain filled pores, can be occasionally seen only in freshly prepared samples, whereas this was very rarely seen with mature filaments in older samples. These measurements make it clear that single APol stabilised OmpF trimers behave like OmpF/APol filaments in preferably attaching to the carbon film on their membrane interacting face. The 1-day-old filaments extended further after (Fig. 3e) 1 week’s total incubation (Fig. 3f). In accordance with these results, it can be concluded that the filaments consist of OmpF trimers bound side by side and mostly seen on their side on the EM grid as in the model shown in Fig. 3b with the long axis of the trimer arranged in line with the filament.

## Conclusion

The results reveal a hierarchy of OmpF self-association which has not been observed in conventional detergents. The SEC almost certainly removes all but directly bound APol from the OmpF trimer, and this is apparently a metastable state. Rather than forming large insoluble aggregates, which form a distinct pellet when centrifuged, the resulting structures are linear filaments of fixed width. The easiest way to imagine how such an array would form is by head to tail stacking of OmpF trimers, but this clearly cannot account for the 6 nm width which corresponds to the height of a trimer. The 10 nm diameter of the trimer most likely lies in the long axis of the filament, and this is supported by the higher resolution LPS-free filaments where a significant beading is observed with an approximate 10 nm repeat. Thus, we propose that the filaments are one dimensional arrays of OmpF linked by their normally membrane exposed surfaces, but why this does not progress to 2D arrays is not clear. Is there a point of specific strong interaction between trimers that overcomes the solubility afforded by APol or does filament formation release enough APol to satisfy the need to stabilise the filaments? The filaments would appear to pre-exist in solution but on contact with the reactive carbon film on the EM grid, preferentially adsorb with one hydrophobic membrane face downwards. Thus, the first step of stabilisation in minimal APol is specific self-association, and the second one we observe is the possible displacement of APol from one face of the filament via contact with the surface. Finally, the OmpF–APol complexes reveal much about the role of LPS in OmpF association. It is known that LPS binds tightly and specifically to OmpF, but here it is shown to strongly favour the assembly of 2D crystals especially in the presence of calcium-induced cross-links. Our previous AFM experiments revealed limited ordered self-association of OmpF in octyl-POE (Cisneros et al. 2006) but the use of APol has revealed a subtlety of interaction which was suppressed by the more conventional detergents. This lateral association into quasi-crystalline arrays has been seen in natural gram-negative OMs by both electron and atomic force microscopy (Hoenger et al. 1993a; Jaroslowski et al. 2009). It suggests that reconstitution of weakly associated membrane complexes may be achieved by careful control of free APol levels.

**Acknowledgments** This work was supported by a Royal Thai Government Scholarship to WA and the Wellcome Trust (Grant number 093581). We thank the Newcastle University Biomedical Electron Microscopy Unit and Dr. Helen Ridley for her technical assistance. We thank Jean-Luc Popot and Christophe Tribet for advice and amphipol samples.

**Open Access** This article is distributed under the terms of the Creative Commons Attribution License which permits any use, distribution, and reproduction in any medium, provided the original author(s) and the source are credited.

## References

- Althoff T, Mills DJ, Popot J-L, Kuehlbrandt W (2011) Arrangement of electron transport chain components in bovine mitochondrial supercomplex I1III2IV1. *EMBO J* 30(22):4652–4664
- Baboolal TG, Conroy MJ, Gill K, Ridley H, Visudtiphohle V, Bullough PA, Lakey JH (2008) Colicin N binds to the periphery of its receptor and translocator, outer membrane protein F. *Structure* 16(3):371–379
- Cao E, Liao M, Cheng Y, Julius D (2013) TRPV1 structures in distinct conformations reveal activation mechanisms. *Nature* 504(7478):113
- Cascales E, Buchanan SK, Duché D, Kleanthous C, Llobès R, Postle K, Riley M, Slatin S, Cavard D (2007) Colicin biology. *Microbiol Mol Biol Rev* 71(1):158–229
- Catoire LJ, Zoonens M, Van Heijenoort C, Giusti F, Guittet É, Popot JL (2010) Solution NMR mapping of water-accessible residues in the transmembrane  $\beta$ -barrel of OmpX. *Eur Biophys J* 39(4):623–630
- Cisneros DA, Muller DJ, Daud SM, Lakey JH (2006) An approach to prepare membrane proteins for single-molecule imaging. *Angew Chem Int Ed Engl* 45(20):3252–3256
- Clifton LA, Johnson CL, Solovyova AS, Callow P, Weiss KL, Ridley H, Le Brun AP, Kinane CJ, Webster JRP, Holt SA, Lakey JH (2012) Low resolution structure and dynamics of a colicin-receptor complex determined by neutron scattering. *J Biol Chem* 287(1):337–346
- Cowan SW, Schirmer T, Rummel G, Steiert M, Ghosh R, Paupit RA, Jansonius JN, Rosenbusch JP (1992) Crystal structures explain functional properties of two *E. coli* porins. *Nature* 358:727–733
- Cvetkov TL, Huynh KW, Cohen MR, Moiseenkova-Bell VY (2011) Molecular architecture and subunit organization of TRPA1 ion channel revealed by electron microscopy. *J Biol Chem* 286(44):38168–38176
- Evans LJA, Cooper A, Lakey JH (1996) Direct measurement of the association of a protein with a family of membrane receptors. *J Mol Biol* 255(4):559–563
- Flötenmeyer M, Weiss H, Tribet C, Popot JL, Leonard K (2007) The use of amphipathic polymers for cryo electron microscopy of NADH:ubiquinone oxidoreductase (complex I). *J Microsc* 227(3):229–235
- Gohon Y, Dahmane T, Ruigrok RWH, Schuck P, Charvolin D, Rappaport F, Timmins P, Engelman DM, Tribet C, Popot J-L, Ebel C (2008) Bacteriorhodopsin/amphipol complexes: structural and functional properties. *Biophys J* 94(9):3523–3537
- Harris JR (1997) Negative staining and cryoelectron microscopy. Bios Scientific Publishers Ltd., Oxford
- Hoenger A, Ghosh R, Schoenenberger CA, Aebi U, Engel A (1993a) Direct in-situ structural-analysis of recombinant outer-membrane porins expressed in an OmpA-deficient mutant *Escherichia coli* strain. *J Struct Biol* 111(3):212–221
- Hoenger A, Pagès J-M, Fourel D, Engel A (1993b) The orientation of porin OmpF in the outer membrane of *Escherichia coli*. *J Mol Biol* 233(3):400–413
- Jaroslowski S, Duquesne K, Sturgis JN, Scheuring S (2009) High-resolution architecture of the outer membrane of the Gram-negative bacteria *Roseobacter denitrificans*. *Mol Microbiol* 74(5):1211–1222

- Johnson CL, Ridley H, Pengelly RJ, Salleh MZ, Lakey JH (2013) The unstructured domain of colicin N kills *Escherichia coli*. *Mol Microbiol* 89(1):84–95
- Lakey JH, Watts JP, Lea EJA (1985) Characterization of channels induced in planar bilayer-membranes by detergent solubilized *Escherichia coli* porins. *Biochim Biophys Acta* 817(2):208–216
- Liao M, Cao E, Julius D, Cheng Y (2013) Structure of the TRPV1 ion channel determined by electron cryo-microscopy. *Nature* 504(7478):107
- Nakae T (1976) Outer membrane of *Salmonella*. Isolation of protein complex that produces transmembrane channels. *J Biol Chem* 251(7):2176–2178
- Nikaido H (2003) Molecular basis of bacterial outer membrane permeability revisited. *Microbiol Mol Biol Rev* 67(4):593
- Popot J-L (2010) Amphipols, nanodiscs, and fluorinated surfactants: three nonconventional approaches to studying membrane proteins in aqueous solutions. In: Kornberg RD, Raetz CRH, Rothman JE, Thorner JW (eds) *Annual review of biochemistry*, vol 79., pp 737–775
- Popot JL, Berry EA, Charvolin D, Creuzenet C, Ebel C, Engelman DM, Flotenmeyer M, Giusti F, Gohon Y, Herve P, Hong Q, Lakey JH, Leonard K, Shuman HA, Timmins P, Warschawski DE, Zito F, Zoonens M, Pucci B, Tribet C (2003) Amphipols: polymeric surfactants for membrane biology research. *Cell Mol Life Sci* 60(8):1559–1574
- Rosenbusch JP (1974) Characterisation of the major envelope protein from *Escherichia coli*. *J Biol Chem* 249:8019–8029
- Schabert FA, Engel A (1994) Reproducible acquisition of *Escherichia coli* porin surface topographs by atomic-force microscopy. *Biophys J* 67(6):2394–2403
- Schneck E, Schubert T, Konovalov OV, Quinn BE, Gutschmann T, Brandenburg K, Oliveira RG, Pink DA, Tanaka M (2010) Quantitative determination of ion distributions in bacterial lipopolysaccharide membranes by grazing-incidence X-ray fluorescence. *Proc Natl Acad Sci USA* 107(20):9147–9151
- Tribet C, Audebert R, Popot J-L (1996) Amphipols: polymers that keep membrane proteins soluble in aqueous solutions. *Proc Natl Acad Sci USA* 93(26):15047–15050
- Tribet C, Audebert R, Popot JL (1997) Stabilization of hydrophobic colloidal dispersions in water with amphiphilic polymers: application to integral membrane proteins. *Langmuir* 13(21):5570–5576
- Tribet C, Mills D, Haider M, Popot JL (1998) Scanning transmission electron microscopy study of the molecular mass of amphipol cytochrome b(6)f complexes. *Biochimie* 80(5–6):475–482
- Visudtiphole V, Thomas MB, Chalton DA, Lakey JH (2005) Refolding of *Escherichia coli* outer membrane protein F in detergent creates LPS-free trimers and asymmetric dimers. *Biochem J* 392:375–381
- White SH (2009) Biophysical dissection of membrane proteins. *Nature* 459(7245):344–346
- Zoonens M, Catoire LJ, Giusti F, Popot JL (2005) NMR study of a membrane protein in detergent-free aqueous solution. *Proc Natl Acad Sci USA* 102(25):8893–8898
- Zoonens M, Giusti F, Zito F, Popot J-L (2007) Dynamics of membrane protein/amphipol association studied by forster resonance energy transfer: implications for in vitro studies of amphipol-stabilized membrane proteins. *Biochemistry* 46(36):10392–10404